

## FEATURES OF SHOCK WAVE FORMATION IN SOFT MATERIALS GENERATED BY IMPACT OF A PLATE

N. Kh. Akhmadeev and R. Kh. Bolotnova

UDC 534.211:539.42:539.63

1. In shock-wave experiments using a scheme of flat impact of plates it is traditional to use as a striker a plate whose material stiffness is coincident with or less than that of the target material which creates from the start a rectangular compression wave in the test target (by stiffness we mean the material acoustic resistance or impedance  $z = \rho c$ ). Use of stiffer material for the striker compared with that of the target leads to a marked change in the flow picture and formation of a compression wave of stepped shape [1]. Consideration of these phenomena has produced the possibility of using soft materials, i.e., porous, polymer, composite, as objects of shock loading. Different approaches to analyzing the passage of shock waves in layered materials have been developed in [1-5]. In [1] transformation of a shock wave under the action of glancing detonation on bimetallic plates was considered, and in [2] it was considered as a result of forming a new stiffer phase. Shock wave evolution in a layered system was studied in [3, 4] and in [4] there was also consideration of forming a zone of discontinuities (a zone with microdamage) in low-strength materials (rubber) with reflection of a shock wave from a backing with lower stiffness. A feature of studies performed in [4] was that the region in which a damage zone formed with tension was recorded as material having zero stiffness. Work in [5] was devoted to shock-wave action on ceramics between aluminum and copper plates with consideration of spalling failure. There acoustic classification is provided for shock and unloading waves in layers whose thickness was varied.

The aim of this work is a study of the mechanism of shock wave formation in targets with low stiffness within the scope of an acoustic approximation and methods for controlling the shape of the wave profile using facing screens.

2. The method of  $p$ - $u$ -diagrams [6] is used below in analyzing the wave picture. We assume that at the instant of impact the immobile target plate of length  $L$  consists of  $n$  layers characterized by the following parameters (a plane unidimensional approximation is considered):  $l_i, \rho_i, c_i, u_i = 0, p_i = 0$  (the lower index  $i = 1, 2, 3, \dots, n$  corresponds to the number of the  $i$ -th layer), and the striker plate flying from the left is single-layer with parameters  $l_0, \rho_0, c_0, u_0 = u_0^0, p_0 = 0$ , where  $\rho_i$  is density,  $c_i$  is speed of sound,  $u_i$  is mass velocity,  $p_i$  is pressure,  $l_i$  is length of the striker ( $i = 0$ ) or target ( $i = 1, \dots, n$ ), and  $L = \sum_{i=1}^n l_i$ . It is assumed that the target has sufficient length ( $L \gg l_0$ ) and during flow picture formation

wave reflected from the rear free surface of the target do not participate.

We write the equation of the shock adiabat in the form [6]

$$(p - p^{(0)})(1/\rho^{(0)} - 1/\rho) = (u - u^{(0)})^2, \quad (2.1)$$

where  $\rho$  and  $u$  relate to the condition in a shock jump. It is noted that the upper index in brackets will denote the number of the substance condition. In particular a zero value for the upper index  $p^{(0)}, u^{(0)}$  correspond to a zero condition. In the case of weak shock waves for which it is possible to use acoustic analysis shock adiabat (2.1) is replaced by the tangent to its initial point  $p^{(0)}, u^{(0)}$ , i.e., at its center. By differentiating (2.1) it is possible to obtain

$$(p - p^{(0)})^2 = (\rho^{(0)} c^{(0)})^2 (u - u^{(0)})^2.$$

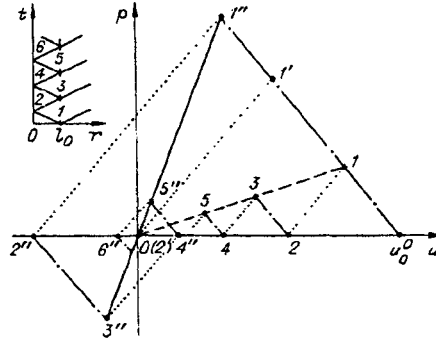


Fig. 1

Here it is possible to note that in a linear approximation shock and unloading wave adiabats coincide and for right- and left-travelling waves they are written as

$$p \pm z^{(0)}u = p^{(0)} \pm z^{(0)}u^{(0)}. \quad (2.2)$$

It follows from (2.2) that the adiabat in the  $p$ - $u$ -plane consists of two branches, i.e., right-hand and left-hand intersecting at its center at an angle governed by stiffness  $z$ . The notation in Eq. (2.2) is simplified assuming that acoustic impedance  $z = \rho c$  is constant and it is determined by density and sound velocity  $\rho^{(0)}$  and  $c^{(0)}$  with initial conditions, and in future for  $z$  we omit the upper indices.

After plate impact both in the target and in the striker shock waves form which propagate in opposite directions. Finding the new state of plates after the shock wave reaches the boundaries of the plate which may be free, stiff, or interlayer (or in the internal flow region) is reduced to determining the point of intersection of the corresponding adiabats on the  $p$ - $u$ -diagram. Here and subsequently we consider two types of interlayer joints: 1) a contact boundary not having a breaking strength, i.e., neighboring layers are laid up or impacted without subsequent adhesion; 2) a boundary whose strength is not less than that of the layers in contact which is achieved by glueing or welding. It is assumed that tensile stresses which arise during unloading do not break the layer material or interlayer joints.

We turn to the  $p$ - $u$ -diagram (Fig. 1) and we consider evolution of the striker and target states during passage of compression and rarefaction waves. On the  $p$ - $u$ -diagram the state will be labelled by the numbers 1, 2, 3, ..., and state 0 relates to the initial target condition, but the point labelled  $u_0^0$  is the initial condition of the striker.

On the  $p$ - $u$ -diagram it is convenient to adopt the following labelling for different condition of the pair of plates being analyzed labelled in Fig. 1 with numbers: an upper index in the form of a prime ( $p'$ ,  $u'$ ) corresponds to a version of the impact of plates made of materials with identical acoustic impedances ( $z_1 = z_0$ ), an index in the form of two primes ( $p''$ ,  $u''$ ) corresponds to a soft striker and a stiff target ( $z_1 > z_0$ ), and absence of an upper index corresponds to a stiff striker and a soft target ( $z_1 < z_0$ ). Here it is assumed that in all of the problems in question target material is varied and the initial striker parameters are assumed to be unknowns ( $l_0, c_0, \rho_0, u_0^0, p_0$  are constants). For this in order to distinguish the direction of wave movement we mark the adiabats of right-travelling waves in the target by dotted lines with  $z_1 = z_0$ , by solid lines with  $z_1 > z_0$  (stiff target), and by dashed lines with  $z_1 < z_0$  (soft target). In the striker the adiabats for right- and left-travelling waves are correspondingly shown by dotted and dashed and dotted lines for all types of the pairs of plates in question.

If a striker in the initial instant has the parameters  $p_0^{(0)}$ ,  $u_0^{(0)}$  and for the target  $p_1^{(0)}$ ,  $u_1^{(0)}$ , then the jump in general condition 1 realized in the striker is represented in Fig. 1 by points 1, 1', 1''. Depending on the ratio of stiffnesses  $z_1$  and  $z_0$  for the impacted plates condition  $p^{(1)}$ ,  $u^{(1)}$  at point 1 is found by solving a set of equations

$$p^{(1)} - z_1 u^{(1)} = p_1^{(0)} - z_1 u_1^{(0)}, \quad p^{(1)} + z_0 u^{(1)} = p_0^{(0)} + z_0 u_0^{(0)},$$

obtained on the basis of relationship (2.2). A minus sign is chosen for the impact adiabat relating to the target since the wave travels to the right, and for the striker a plus sign is chosen (the wave propagates to the left). For the problem formulated above by specifying pressure and mass velocity at the initial instant of impact ( $p_1^{(0)} = 0$ ,  $u_1^{(0)} = 0$ ,  $p_0^{(0)} = 0$ ,  $u_0^{(0)} = u_0^0$ ) we obtain

$$p^{(1)} = \frac{z_0 z_1}{z_0 + z_1} u_0^0, \quad u^{(1)} = \frac{z_0}{z_0 + z_1} u_0^0. \quad (2.3)$$

The unloading condition in the striker which forms after emergence of the compression wave at its free surface may be determined on the  $p$ - $u$ -diagram by finding the point of intersection of the shock adiabat of the striker in condition  $p^{(1)}, u^{(1)}$  with straight line  $p = 0$  (abscissa axis), i.e., by solving the set of equations

$$p^{(2)} - z_0 u^{(2)} = p^{(1)} - z_0 u^{(1)}, \quad p^{(2)} = 0.$$

Considering the values of  $p^{(1)}$  and  $u^{(1)}$  from (2.3) we have

$$p^{(2)} = 0, \quad u^{(2)} = \frac{z_0 - z_1}{z_0 + z_1} u_0^0,$$

which corresponds to points 2, 2', 2" in Fig. 1. Consequently, with coincidence of stiffness for the striker and the target when  $z_1 = z_0$  we have  $p^{(2)} = 0, u^{(2)} = 0$  which determines the point of origin of the coordinate (2'). In the case of a stiff target when  $z_1 > z_0$  the striker acquires a negative mass velocity. This point is shown by 2"; if a stiff target is used ( $z_1 < z_0$ ) the mass velocity of the striker at point 2 is positive and  $u^{(2)} < u^{(1)}$ . The unloading wave front in the striker moving from the free surface towards the impact surface at the instant of passing the contact boundary creates condition 3. For convenience in the left-hand part of Fig. 1 a fragment of the  $r$ - $t$ -diagram is presented ( $r$  is Lagrangian coordinate,  $t$  is time) in which the compression and unloading wave fronts are shown and the conditions realized in the striker and the target are labelled with numbers. Then the target material is stiffer ( $z_1 \geq z_0$ ) the striker rebounds from the target with velocity  $u^{(2')}$ . The condition in the striker at the instant of rebound will be determined on the  $p$ - $u$ -diagram (Fig. 1) by point 2" obtained as noted above with intersection of the shock adiabat of the striker and straight line  $p = 0$ . Rebound of the striker will be completed with formation of a rectangular compression wave profile in the target. If with interaction of the striker with the target there was adhesion of the plates, for example welding of the [7], the unloading wave in the striker causes at the contact boundary with the target a new condition determined by point 3". In the case of a soft target ( $z_1 < z_0$ ) the condition at the contact boundary will be determined by point 3. Pressure  $p^{(3)}$  and mass velocity  $u^{(3)}$  for all of the pairs of plates in question may be obtained analytically by solving the following set of equations

$$\begin{aligned} p^{(3)} + z_0 u^{(3)} &= p^{(2)} + z_0 u^{(2)}, \\ p^{(3)} - z_1 u^{(3)} &= p^{(2)} - z_1 u^{(2)}. \end{aligned} \quad (2.4)$$

Set (2.4) is obtained from (2.2) taking account of the movement directions for waves in plates. The solution of (2.4) has the form

$$p^{(3)} = \frac{z_0 z_1 (z_0 - z_1)}{(z_0 + z_1)^2} u_0^0, \quad u^{(3)} = \frac{z_0 (z_0 - z_1)}{(z_0 + z_1)^2} u_0^0. \quad (2.5)$$

From relationships (2.5) for  $p^{(3)}$  and  $u^{(3)}$  it follows that if  $z_1 = z_0$ , then  $p^{(3)}$  and  $u^{(3)}$  equal zero. This means that in the target beyond the first step of the shock wave there is no disturbance. In the case of a stiff target with  $z_1 > z_0$  in the striker-target contact zone tensile stresses arise determined by condition 3", and for a soft target with  $z_1 < z_0$  at the instant of arrival of the unloading wave from the direction of the striker a region of compressive stresses is maintained specified by point 3 (see Fig. 1). Consequently, for a soft target rebound of the striker is not observed and during reflection of the wave from the contact surface the striker and target will be in a condition of compression.

The process of partial unloading described at the contact boundary will be repeated periodically and a compression wave will form in the target with a stepwise decreasing amplitude at the unloading front as shown in Fig. 2 (see wave profiles labelled  $p^{1*}$  and  $p^{3*}$ ). The condition arising in the target is shown in Fig. 1 by points 3, 5, etc. Absence of tensile stresses in soft targets is noted in [1, 7] where there is analysis of shock-wave flow in two-layer targets connected with studying welded joint quality with explosive welding.

Using the solution of  $p^{(3)}$  and  $u^{(3)}$  of set (2.5) we provide expressions for pressure and mass velocity for the  $(2k - 1)$ -th ( $k = 1, 2, \dots$ ) step of the rear front of the compression wave, i.e., for points with uneven numbering and identical upper indexing on the  $p$ - $u$ -diagram in Fig. 1 (for example  $k = 2$  corresponds to point 3):

$$\begin{aligned} p^{(2k-1)} &= \frac{z_0 z_1 (z_0 - z_1)^{k-1}}{(z_0 + z_1)^k} u_0^0, \\ u^{(2k-1)} &= \frac{z_0 (z_0 - z_1)^{k-1}}{(z_0 + z_1)^k} u_0^0. \end{aligned} \quad (2.6)$$

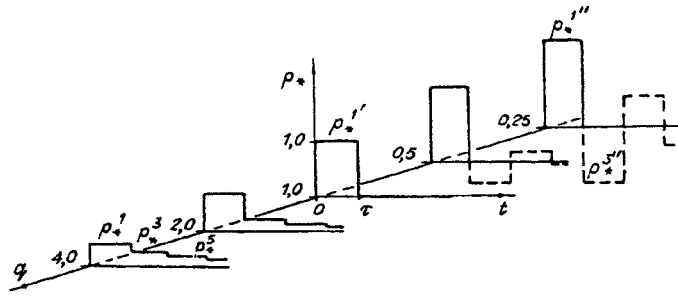


Fig. 2

From general Eqs. (2.6) it follows that if the stiffnesses of the striker and target coincide ( $z_1 = z_0$ ) only the first step of the compression wave arises and then there is no disturbance, i.e., we have

$$\begin{aligned} p^{(k)} &= z_0 u_0^0 / 2, & u^{(k)} &= u_0^0 / 2 & \text{for } k = 1, \\ p^{(k)} &= 0, & u^{(k)} &= 0 & \text{for } k > 1. \end{aligned}$$

It is of interest to evaluate the effect of the ratio of striker and target stiffnesses on compression wave amplitude and the form of the unloading wave. As in [8] for convenience we introduce a relative value  $q = z_0/z_1$ . Within the scope of the notation adopted Eqs. (2.6) are transformed to

$$p^{(2k-1)} = \frac{z_0(q-1)^{k-1}}{(q+1)^k} u_0^0,$$

$$u^{(2k-1)} = \frac{(q-1)^{k-1}}{(q+1)^k} u_0^0.$$

For dimensionless pressure  $p_*^{(2k-1)}$  normalized relative pressure  $p = z_0 u_0^0 / 2$  (equal to compressive pressure which arises with impact of plates of identical materials with stiffness  $z_1 = z_0$ , i.e., with  $q = 1$ , and a corresponding pressure in condition 1' on the  $p$ - $u$ -diagram in Fig. 1), it is possible to write

$$p_*^{(2k-1)} = \frac{2(q-1)^{k-1}}{(q+1)^k} \text{ for } q > 1. \quad (2.7)$$

It is noted that if  $q = 1$ , then  $p^{(1)} = 1$  and  $p^{(k)} = 0$  for  $k > 1$ . From (2.7) it emerges immediately that  $|p_*^{(2k+1)}| < |p_*^{(2k-1)}|$

Presented in Fig. 2 are compression wave profiles with subsequent unloading at the contact boundary realized during impact of a striker and target for different values of relative stiffness  $q = 0.25, 0.5, 1.0, 2.0, 4.0$ . For clarity in Fig. 2 axis  $q$  is given on a longitudinal scale. With coincidence of striker and target material stiffnesses ( $q = 1$ ) the compression wave as a result of rebound of the striker has a rectangular shape with amplitude  $p^{(1)*} = 1$ . If plates impact with relative stiffness  $q < 1$  (stiff target version) then the compression wave amplitude increases.

In the case of stiff adhesion of striker and target (the second type of interlayer joint) behind the first compression wave there follows a tension wave of lower amplitude, then again a compression wave, etc., and then the stiffer the target, the greater is the amplitude of the compression and tension waves and the more rapidly they fade (see pressure profiles in Fig. 2 with  $q = 0.5$  and  $0.25$  marked by a broken line). In the limiting case when  $q = 0$ , which corresponds to impact of a plate on a stiff wall ( $z_1 = \infty$ ) there is doubling of the amplitude of the first compression wave behind which in the case of striker adhesion there follows a tension wave of equal amplitude after which the flow picture will be periodically repeated.

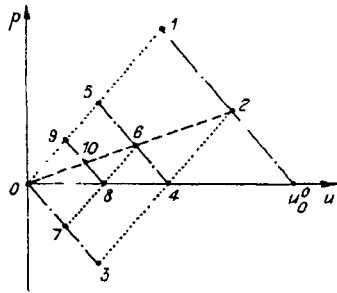


Fig. 3

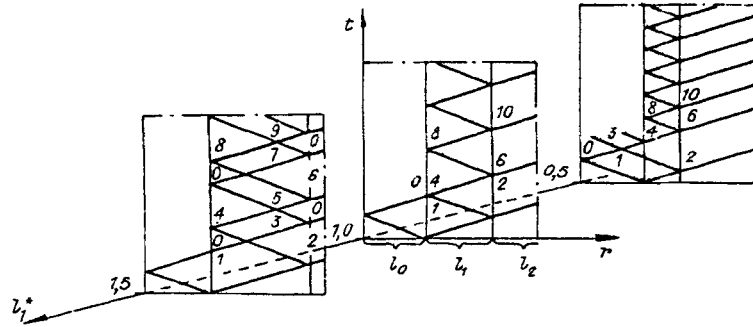


Fig. 4

We consider a version when the relative stiffness  $q > 1$  (stiff striker and soft target). From data in Fig. 2 it is possible to see that an increase in  $q$  ( $q = 2.0, 4.0$ ) leads to formation of a compression wave with lower amplitude and smoother unloading of it.

It is possible to show that the sum of pressures for all steps of the wave formed for any positive  $q > 0$  with  $k \rightarrow \infty$  is the same and equals  $p$ . In fact, by summing the pressures in all steps we obtain

$$\begin{aligned} \sum_{k=1}^{\infty} p_*^{(2k-1)} &= \frac{2}{q+1} + \frac{2(q-1)}{(q+1)^2} + \frac{2(q-1)^{k-1}}{(q+1)^2} + \dots \\ &= \frac{2}{q+1} \left[ 1 + \frac{q-1}{q+1} + \dots + \left( \frac{q-1}{q+1} \right)^{k-1} + \dots \right] = 1. \end{aligned} \quad (2.8)$$

Since series  $\sum_{k=1}^{\infty} p_*^{(2k-1)}$  is an infinite geometric progression, then it converges absolutely with  $\left| \frac{q-1}{q+1} \right| < 1$ , i.e.,  $q > 0$ :

$$\sum_{k=1}^{\infty} p_*^{(2k-1)} = p = z_0 u_0^0 / 2.$$

3. In solving certain practical problems in the case of impact of a stiff striker with a soft target ( $z_1 > z_0$ ) as a rule only the first step of the shock wave which forms is considered [8] and the contribution of the subsequent step is assumed to be small. We introduce into consideration the value (called pulse pressure)  $P = p\tau$ , where  $p$  is pressure in the shock-wave front,  $\tau$  is its duration. According to the solution (2.8) the overall pressure pulse for the shock wave

$$P^{\Sigma} = \sum_{k=1}^{\infty} p_*^{(2k-1)} \tau = 0,5 z_0 u_0^0 \tau$$

( $\tau = 2l_0/c_0$ ), and the pressure pulse of its first step in accordance with (2.3)

$$P^{(1)} = \frac{z_0 z_1}{(z_0 + z_1)} u_0^0 \tau.$$

Then  $\Delta P$  for the negligible part of the shock wave is determined by the expression

$$\Delta P = P^{\Sigma} - P^{(1)} = \frac{z_0 u_0^0 (z_0 - z_1) \tau}{2(z_0 + z_1)}. \quad (3.1)$$

We assume that failure to consider pressure pulse  $\Delta P$  will have little effect on the wave picture of flow if  $\Delta P$  is 0.25 or less of the pressure pulse of the first step  $P^{(1)}$ . As is easy to show from (3.10) this is achieved when the target material stiffness satisfies the relationship  $0.5z_0 \leq z_1 < z_0$ . If negligible value  $\Delta P$  decreases (for example it is assumed that  $\Delta P = 0.125P^{(1)}$ , then target material stiffness  $z_1$  should increase and it will be determined by the inequality  $0.8z_0 \leq z_1 < z_0$ . Whence it follows that for materials for which formation of an extended compression wave is typical it is not possible to discard the steps of the compression wave following the first and it is necessary to carry out additional analysis.

The question arises whether it is possible to obtain an isolated compression wave in soft targets by use of a stiff facing layer. In order to analyze the situation which arises it is also convenient to draw on the  $p-u$ -diagram method. Shown in Figs. 3-5 is the process of impact loading for a two-layer target in the form  $p-u$ -,  $r-t$ -, and  $p^*-t$ -diagrams respectively. The  $r-t$ -

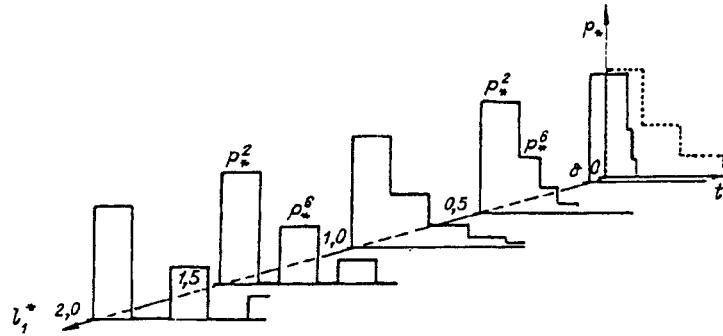


Fig. 5

and  $p^*-t$ -diagrams are given in several versions depending on dimensionless thickness for the facing layer of the target  $l_1^*$  ( $l_1^* = l_1/l_0$ ). It is assumed that the main layer of the target as previously has sufficient length ( $l_2 \gg l_1, l_0$ ). We consider the problem of the effect of a thin facing layer. We assume that the stiffness of the striker and target facing layer material coincides and the material of the main layer is softer, i.e.,  $z_0 = z_1 > z_2$ , and for the thickness of the layers there is the relationship

$$l_1/c_1 < l_0/c_0 \ll l_2/c_2. \quad (3.2)$$

This condition is determined as follows: the thickness of the facing layer is selected so that the time of shock wave travel through the facing layers less than the time of wave travel through the striker. For simplicity we assume that  $c_0 = c_1$ , then from (3.2) it emerges that  $l_1^* < 1$ . At the instant of impact at the impact boundary a condition is realized labelled with 1 in Figs. 3 and 4. After rebound of the striker there is a new condition labelled by point 0 in the striker and by point 4 in the facing layer.

The interlayer boundary in the target will generate a shock wave of stepped form in which the pressure of each step is determined by conditions labelled in the  $p-u$ -diagram in Fig. 4 by 2, 6, 10, etc. For example, condition 2 is obtained by intersection of the left-hand branch of the facing layer adiabat with stiffness  $z_1 = z_0$  which is in condition 1, and the right-hand branch of the target adiabat with stiffness  $z_2$  emerging from point 0 (see section 0-2). Consequently, the process of compression wave formation occurs similar to the case of impact of a stiff striker with length  $l_0$  equal to  $l$ , on a soft target. This version is analyzed above (see data in Fig. 1). The difference is that the duration of the first step of the shock wave analyzed depends on striker thickness  $l_0$  and for the rest of the steps it depends on the thickness of the facing layer  $l_1$ . This is seen from data in Fig. 5 where pressure profiles are presented with  $l_1^* = 0.5$ . A reduction in thickness  $l_1$  leads to the situation that the shape of the wave generated will approach rectangular coinciding with the profile of its first step.

This situation is shown in Fig. 5 on the  $p^*-t$ -diagram with  $l_1^* = l_1/l_0 = \delta$ . For the limiting value  $l_1^* = 0$  (absence of a facing layer) the profile  $p^*(t)$  is shown by a dotted line and it coincides with data in Fig. 2 with  $q = 2.0$  and  $0.4$ . In actual experiments determination of the limiting minimum value of  $\delta$  promoting formation in soft materials of a rectangular compression wave will depend on the curvature of its leading front; the stronger blurring of the shock jump, the greater should be the minimum thickness of the facing layer  $\delta$ . An increase in  $l_1^*$  to the value 1 ( $l_1 = l_0$ ) leads to the situation that the duration of the second and subsequent steps of the compression wave formed coincide with the duration of the first step.

Corresponding  $r-t$ -diagrams and pressure profiles are shown in Figs. 3 and 5 with  $l_1^* = 1$ . It is noted that with equal striker and facing layer lengths and stiffnesses in a soft target a shock wave forms identical to a shock wave which forms in target without a facing layer (see Fig. 2 for  $q = 4.0$ ). In fact this ratio of thicknesses for the striker and the first screening layer is as a rule selected in actual experiments [4]. A further increase in facing layer thickness when the condition  $l_0 < l_1 \ll l_2$  ( $l_1^* > 1$ ), is fulfilled leads to the situation that following behind the first compression wave there is a pause of an undisturbed condition depending on  $l_1^*$  (see point 0 in Fig. 3). This may cause rebounding of the facing layer with absence of an adhesion of it with the main layer (the first type of interlayer joint) and thereby accomplish cutting off of the second and subsequent steps of the wave (the profiles described are shown in Fig. 5 with  $l_1^* = 0.5$  and  $2.0$ ). Separation of the facing layer from the main layer is entirely possible since at the instant of separation (see Figs. 3 and 4) the facing layer has a lower mass velocity (condition 3 on the  $p-u$ -diagram than the main plate (condition 2). If rebound of the facing layer does not occur then the pause of an undisturbed condition following the first wave may be controlled by the thickness of the facing layer  $l_1^*$ .

In conclusion we note that acoustic analysis whose procedure is described in this work makes it possible to detail the structure of compression pulses which arise with impact of plates with different stiffnesses. In the case of a soft striker ( $z_1 \geq z_0$ ) as a result its rebound a rectangular compression wave forms (this is a known solution which is used extensively in experimental practice). Stiff adhesion of plates leads to the situation that behind the first compression wave there follows a series of waves of alternating pressure and reducing amplitude. Impact of a stiff striker with a soft target forms a compression wave of stepped shape whose extent and configuration of the unloading front are determined by the ratio of plate stiffnesses. With use of quite thin facing screens whose stiffness coincides with that of the striker in a soft target a compression wave is generated whose shape is close to rectangular. If the lengths of the striker and facing plate are comparable and they consist of identical materials then the stepped compression wave is similar to that which arises without use of a facing layer.

The requirement for detailed analysis of the process of shock wave propagation in soft materials (for example polyethylene, fluoroplastic, various rubbers) arose in numerical studies of wave phenomena in layered materials. Practice showed that with use of continuous counting methods difficulties with the identification of compression and unloading waves generated at contact and interlayer boundaries. Drawing on acoustic analysis made it possible to facilitate markedly evaluation of the wave flow picture and also to reveal its structure and features in specific situations.

The authors thank Academician R. I. Nigmatulin for attention to the work and useful discussion.

## REFERENCES

1. M. S. Kachan, Yu. V. Kiselev, and Yu. A. Trishin, "Interaction of shock waves with contact boundaries of impacting bodies," *Fiz. Goreniya Vzryva*, **11**, No. 5, 767-773 (1975).
2. R. I. Nigmatulin, *Dynamics of Multiphase Materials, Part 1* [in Russian], Nauka, Moscow (1987).
3. V. F. Nesterenko, V. M. Fomin, and M. A. Cheskidov, "Damping of strong shock waves in layered materials," *Prikl. Mekh. Tekh. Fiz.*, No. 4, 130-139 (1983).
4. G. I. Kanel' and A. V. Utkin, "Dynamics of the cavitation region with reflection of a compression pulse from the interface of two materials," *Prikl. Mekh. Tekh. Fiz.*, No. 4, 23-26 (1991).
5. L. H. L. Louro and M. A. Meyers, "Effect of stress state and microstructural parameters on impact damage of alumina-based ceramics," *J. Mater. Sci.*, No. 24, 2516-2532 (1989).
6. A. B. Zel'dovich and Yu. P. Raizer, *Physics of Shock Waves and High Temperature Hydrodynamic Phenomena* [in Russian], Nauka, Moscow (1966).
7. M. S. Kachan and Yu. A. Trishin, "Compression and tension waves with impact of solids," *Fiz. Goreniya Vzryva*, **11**, No. 6, 958-963 (1975).
8. N. Kh. Akhmadeev and R. Kh. Bolotnova, "Effect of facing layer stiffness on reducing tensile stresses in a two-layer composite," *Mekhan. Kompozit. Materialov*, No. 4, 744-746 (1986).